Study of Graphenic Carbon Powder Interaction with TiO2 Grown by RF Sputtering and Effect on the Photocatalytic Activity

Hafeez Ullah, Francesca Marchetti, Nadhira Laidani*

Fondazione Bruno Kessler, Centro Materiali e Microsistemi, Via Sommarive 18, 38123 Trento, Italy
laidani@fbk.eu

TiO2 nanoparticles were deposited by RF sputtering onto powders made of graphenic carbon flakes. The influence of the RF power during the sputtering process was investigated, with a focus on the interaction of this powder with titanium dioxide. i.e. the electron properties change at the interface between the carbon support and the oxide and the structural modifications of the support. X-ray photoelectron spectroscopy was employed for such a purpose. It was found that the C 1s core level binding energy in the graphenic powder shifted to lower binding energies values upon the deposition of the TiO2 nanoparticles. Such a downshift was observed on Ti2p and O1s core levels too and increased with rising of TiO2 amount. The downshift of the C 1s core level indicates a charge transfer from graphene to TiO2 nanoparticles due to the lower work function of carbon relatively to that of TiO2, with a lowering of the Fermi level. The graphenic powder - supported TiO2 nanoparticles showed an improvement of the photocatalytic activity towards methyl red molecule degradation under solar light.

1. Introduction

Recently TiO_2 nanostructures and graphene sheets were extensively studied for the high performance of the photo-catalytic activity of graphene-TiO_2 composite and also to improve other properties of graphene. It has been well established that graphene as a catalyst support has high potential for the improvement of the photocatalytic activity due to its unique properties, such as high surface area, high transparency, high electrical conductivity and good interfacial contact with adsorbents [Park et al. 2008; Kim et al. 2011]. Different chemical and physical approaches were used to prepare the TiO_2 nanostructures onto graphene, such as the one step hydrothermal method for a reduced graphene oxide-TiO_2 nanostructure composite without using reducing agent [Sher Shah et al. 201]. They measured the photocatalytic activity of the prepared composite for the degradation of rhodamine B dye and of a colorless dye like benzoic acid, under visible light. The same method was adopted to obtain a graphene-TiO_2 composite tested for its photocatalytic performance towards the degradation of rhodamine B, methylene blue and methyl orange under UV light irradiation [Gu et al. 2016]. A hydrothermal method used for the preparation of the TiO_2 -graphene composite resulted in a high photocatalytic activity for the degradation of sodium pentachlorophenol [Zhang et al. 2009].

Studies showed that the graphene-TiO_2 composite structure is characterized by particular interface electron properties where a charge transfer occurs. The charge transfer phenomenon between the graphene and TiO_2 has been explained by Du et al. [Du et al. 2011] by using ab initio calculations, the charge being transferred from graphene to TiO_2 as the consequence of large work function difference, which leads to significant hole doping of graphene.

In this work, the results of a study of TiO_2 particle decoration of graphenic carbon powder are presented, with a focus on the modification of the electronic properties of the graphenic powder at the interface with the nanoparticles, the structural changes of the carbon-based powder and on the oxide nanoparticles. The TiO_2 nanoparticles were grown onto graphenic flakes by radio-frequency (RF) sputtering, a "dry" method in contrast with the "wet" method so far generally used. The decorated powder was tested for its photocatalytic activity towards methyl red organic molecule.

2. Experimental details

2.1 Sample preparation

Commercial graphenic powder was purchased in Graphene Supermarket (Grade AO-1). The average flake thickness and lateral size values provided by the supplier were 1.6 nm and 10 μm ca. respectively, with a specific surface area given as (400 – 800) m²/g. Prior and after the oxide deposition, the graphenic powders were handled in a glove box where they were protected from the moisture and other kinds of the contamination. No further powder processing was applied.

2.2 Deposition

The anatase TiO_2 nanoparticles were deposited onto the graphenic powder by RF sputtering in argon plasma. A high purity (99.99 %) 5 cm diameter TiO_2 disc was used as a sputtering target. The distance between the TiO_2 target and graphene powder were fixed at 50 mm. A powder vibration system was used during the deposition process to uniformly decorate the graphene powder with TiO_2 nanoparticles. The RF power was varied between 30 W and 80 W, corresponding to a target self-bias voltage in a range between -174 and -294 V. The process pressure and the powder vibration frequency and amplitude were kept constant at 6 Pa and 20 Hz and 32μm respectively. The deposition time was fixed at 40 min.

2.3 Characterization

X-ray photoelectron spectroscopy (XPS) analysis was performed with a Scienta 200 instrument, using a monochromatic AlKα X-ray source (1486.6 eV). The high-resolution (0.4 eV) spectra of C1s, O1s and Ti2p core lines were acquired at 150 eV pass energy. The binding energies (BEs) were referenced to the Fermi level. The core line spectra were fitted with a Gauss-Lorentz peak shape, after a Shirley-type background subtraction, using a software based on RStudio [Speranza and Canteri 2019]. The atomic ratio values between elements were determined from the area ratio of selected core level peaks corrected by the sensitivity factors of the latter.The sample morphology before and after decoration was investigated by transmission electron microscopy (TEM).

2.4 Photo-activity test

The photocatalytic activity of the decorated powder was studied by measuring the degradation kinetics of methyl red (MR) molecules in a solution of 16 µM MR in presence of an 8mM Tris-HCl buffer (pH 8.2). Quartz cuvettes containing 2.55 ml suspensions (with a powder concentration of 23,3 μg/ml) were placed over a waving platform shaker to allow the solution to get in contact with the powder surface and to avoid the sedimentation of the powder over time. The solutions received perpendicularly the light irradiation from a solar simulator set at the power of 1 sun (1 kW/m2). The absorbance spectra of the methyl red solutions are acquired over the UV–Visible range (200–800 nm) using a Cary 100 spectrophotometer, after regular time intervals. To monitor the dye degradation kinetics, the absorbance value at 430 nm wavelength (corresponding to maximum absorbance of the MR molecule in the visible light range) was followed.

3. Results and Discussion

By the variation of the RF power values, different amounts of TiO_2 nanoparticles onto graphene were obtained. The influence of the TiO_2 concentrations on the chemical and electronic properties of the graphenic sheets is discussed. The morphology of the decorated powder and its interaction with the TiO_2 nanoparticles were characterized by TEM and XPS respectively.

3.1 Surface morphology of the decorated graphene with sputtered TiO_2

Figure1 shows the decorated graphene with TiO_2 nanoparticles deposited at 80 W, as acquired by TEM analysis. Very small TiO_2 nanoparticles anchored onto graphene can be observed. Graphene sheets were decorated with a high coverage of TiO_2 nanoparticles and the deposited particles are well distributed over the graphene sheets. The size of the deposited TiO_2 nanoparticles was in the range of (5-10) nm. For such specimen, approximately 75% of the powder surface was covered by the oxide.
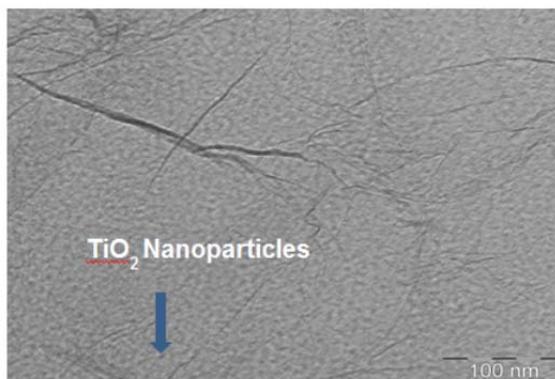
Figure 1: TEM image of deposited TiO2 nanoparticles onto the graphenic sheets composing the powder.

3.2 XPS analysis undoped graphene and TiO$_2$ doped graphene deposited at different RF power values

The high resolution XPS spectra of the C 1s core level of the undecorated and decorated powder with TiO$_2$ nanoparticles deposited at different power values are shown in Figure 2(a). The C 1s core level spectra were fitted by three components, centred at the following BE: 284.45, 285.23 and 286.2 eV, which are attributed to C-C (sp^2), C-H/C-C (sp^3) and C-O bonds respectively. It was observed that the C 1s core level of the graphene shifted toward lower BE values by depositing TiO2 nanoparticles onto the powder. The main component relative to sp^{2}C-C bonding shifted by -0.04 eV for a 30W power and continued down-shifting by raising the RF power values to reach -0.17 eV for 80 W.
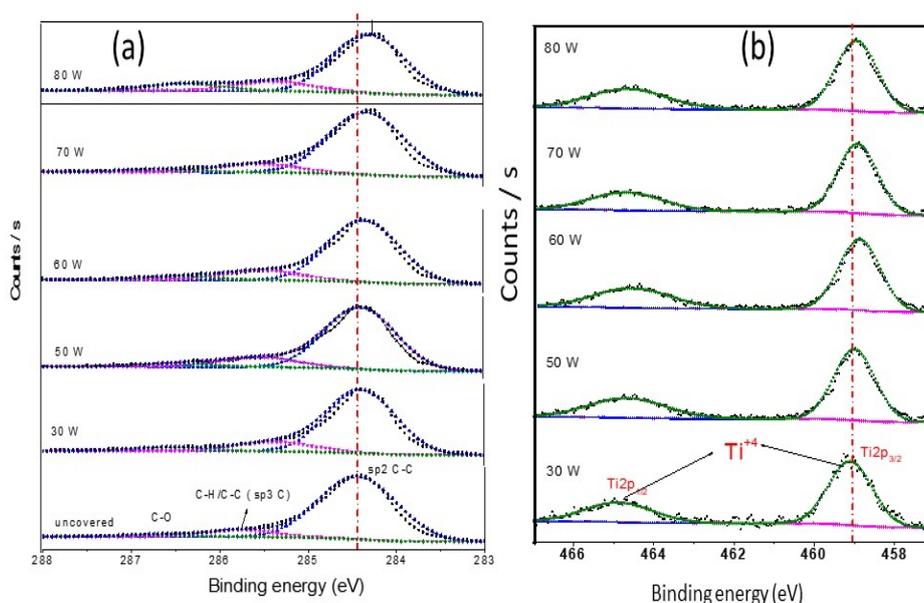

Figure 2: XPS spectra for graphenic powder and deposited TiO$_2$ nanoparticles at different RF power values (a) C 1s core levels with marked positions of the C-C (sp2) bond (b) Ti 2p core level spectra.

The BE reduction of the C 1s core level after the deposition of TiO$_2$ nanoparticles can be understood as a p-doping of the graphenic sheets, whereas the electrons are transferred from graphene to TiO$_2$ nanoparticles at the interface, resulting in a lowering of the Fermi level in the graphene sheets. Recently it was reported that due to the interaction of graphene with a high band gap semiconductor, the C 1s core level binding energy reduced to lower values due to the charge transfer at the interface in order to align the Fermi level and to the difference of the work function values [Joucken et al. 2014; Geng et al. 2008]. Similar observation about the charge transfer between graphene and TiO$_2$ due to large difference in work function values between the TiO$_2$ (5.50 eV) and graphene (4.3 eV) is reported by Du et al, using density function theory [Du et al. 2011].

The Ti 2p spectra for the decorated powder at different RF power values are presented in Figure 2(b), showing the peak fitting by two components, at 459.08 eV and 464.95 eV corresponding to Ti 2p$_{3/2}$ and Ti

$2p_{1/2}$ in TiO_2 (Diebold 2003). Similar to the C1s spectra, with increasing the RF power values, the Ti 2p peaks shifted towards the lower binding energy values, with a maximum downshift of - 0.26 eV for 80 W.

Figure 3(a) depicts the O 1s spectra for the deposited TiO_2 nanoparticles onto the graphenic powder at different power values. The O 1s XPS spectra were fitted by three components, the main one located at 530.7 eV BE and assigned to O^{-2} bound to Ti^{+4} [Safeen 2015]. Two minor components, located at 532.12 eV and 533.3 eV, can be attributed to the C–OH and C-O bonds respectively [Luciu 2012a; Luciu et al. 2012b].

The atomic ratio Ti/C determined as the area ratio between the main C1s component and the $Ti2p_{3/2}$ peak, corrected by the corresponding sensitivity factor. Similarly, the oxide stoichiometry (O/Ti) was measured on the basis of the area under the main component of the O1s spectra and that under the Ti $2p_{3/2}$ component. The Ti/C and the O/Ti, atomic ratios are plotted in function of the applied RF power in Figure 3 (b), where it can be observed the increase of Ti/C with the RF power increase and the O/Ti decrease from 1.96 to 1.86 when the applied power raised from 30 W to 80 W. The deposited oxide grew more oxygen deficient at high RF power values.
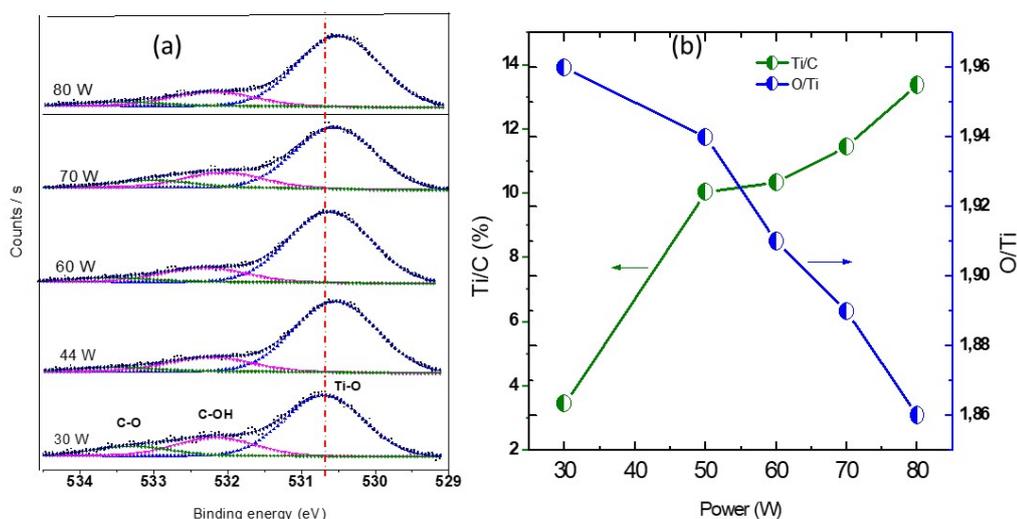

Figure 3: XPS O 1s core peak of decorated graphenic powder(a) and variations of Ti /sp^{2}C and O/Ti atomic ratio (oxide stoichiometry in function of the applied RF power for sputtering (b).

3.3 Photocatalytic activity of the decorated powder

The photocatalytic activity study of the undecorated and decorated graphenic powder with TiO_2 nanoparticles with an atomic ratio (Ti/C sp^2 = 13.4 at.%) grown at 80 W was carried towards methyl red (MR) dye degradation as a model reaction under simulated solar light.

Figure 4(a) shows the photo catalytic activity in terms of the variation of the MR concentration, (C), in the test solution in function of the exposition time to solar light, normalized to the initial concentration at time t=0 (C_0). This normalized concentration (C/C_0) is taken equal to the normalized MR absorbance to the initial absorbance at time t=0, (A/A_0).

It was observed that the variation of the degradation level of MR molecules in presence of the graphenic powder is comparable to that of MR itself (within the ± 0,025 error limits), implying that the powder had no intrinsic catalytic activity. The degradation of MR was enhanced in the presence of the powder-TiO_2 composite, containing 13.4 at.% Titanium oxide by about 30%. According to a first-order degradation kinetics at low dye concentration [Al-Ekabi and Serpone,1988], following the equation $C/C_0 = e^{-kt}$, the rate constant k can be determined by plotting $Ln(C/C_0)$ in function of time (Figure 4(b)). It was found equal to 1.5×10^{-3} min^{-1} for the TiO_2/graphenic powder sample obtained with 80W power. For comparison and assuming the same kinetics regime for a 75 nm continuous TiO_2 film onto a silicon substrate, tested in the same MR solution conditions, a value of $k=1,73 \times 10^{-4}$ min^{-1} was found.

It is reported that three factors are important for the photocatalytic process, that is, the charge separation and transportation, absorption of light and the adsorption of the pollutant molecules [Yang et al. 2016]. In relation of the present graphenic powder-TiO_2 composite, it was also reported that the formation of the charge transfer complex at the interface of the oxide and graphene sheets would be expected to facilitate the photocatalytic activity under UV-Vis light, by facilitating a more effective charge separation between electrons and the holes

created by the electron excitation, and reducing e-hole recombination events [Park et al. 2009; Seo et al. 2005]. Furthermore, the present XPS results showed that the deposited oxide nanoparticles were under-stoichiometric, (best described as TiO_{2-x}). It is well assumed that such oxygen vacancies in the TiO_2 nanoparticle can enhance the photocatalytic activity of the TiO_2. The oxygen vacancies in the TiO_{2-x} generate localized states within the band gap, ranging from 0.75 to 1.18 eV below the conduction band and were reported to lead to a photo-response to the light irradiation [Emeline et al. 2008].

The contribution of graphenic carbon to the photocatalytic activity of TiO_2 may be explained by the offered higher specific surface area, the more conductive nature and the lower work function of the graphenic carbon powder and the higher absorbance in the visible part of the solar spectrum. However, these characteristics are not exclusively pertaining to graphenic carbon but to other carbon forms too. In fact, this question was initially addressed by Zhang et al. [Zhang et al. 2010] as to whether the role of graphene in enhancing TiO_2 photoactivity is fundamentally different from that of carbon nanotubes, fullerene and activated carbon, pointing towards rather a negative answer. More investigation, by taking into account all the complexity and intercorrelation of the key parameters influencing the photocatalytic activity, as well as the structure (such as disorder, defects, doping) of the considered graphenic carbon itself, is still needed to answer this question.
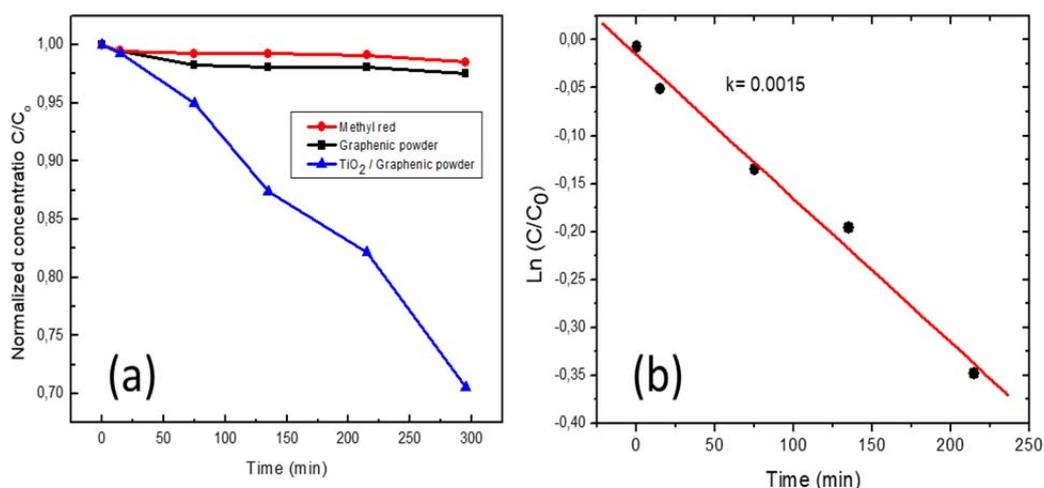

Figure 4: (a) Normalized dye concentration (C/C_0) time variation under solar light exposure of decorated graphenic carbon powder with TiO_2 nanoparticles at 80 W, uncoated powder and methyl red (b) $Ln(C/C_0)$ - Time plot for the determination of the rate constant as the slope of the data linear fit, for the powder decorated at 80 W.

4. Conclusion

The influence of the TiO_2 concentration on the chemical and photocatalytic activity of the decorated graphene sheets was discussed. The particle nature of the deposited TiO_2 was confirmed by TEM examination. The XPS analysis further showed the p-doping of graphene upon the deposition of the TiO_2 nanoparticles, whereas the C 1s core level binding energy downshift was evidenced. The well dispersed TiO_2 nanoparticles onto the graphenic powder used as a catalyst support showed photocatalytic activity towards MR degradation.

Acknowledgments

References

Al-Ekabi H., Serpone N., 1988), Photocatalytic degradation of chlorinated phenols in aerated aqueous solutions over TiO_2 supported on a glass matrix, Journal of Physical Chemistry 92(20), 5726-5731.
Diebold U., 2003, The surface science of titanium dioxide, Surface Science Reports 48, 53–229.

Du A., Hau Ng Y. H., Bell N. J., Zhu Z., Amal R, and Smith S. C., 2011, Hybrid graphene/titania nanocomposite: interface charge transfer, hole doping, and sensitization for visible light response. The Journal of Physical Chemistry Letters 2, 894-899.

Emeline A. V., Kuznetsov V. N., Rybchuk V. K. and Serpone N, 2008, Visible-light-active titania photocatalysts: the case of N-doped TiO_2s—properties and some fundamental issues, International Journal of Photoenergy, 1-19.

Geng H.-Z., Kim K. K, Song C., Xuyen N. T., Kim S. M., Park K. A., Lee D. S., An K. H., Lee Y. S., Chang Y., Lee Y. J., Choi J. Y., Benayad A. and Lee Y. H. , 2008, Doping and de-doping of carbon nanotube transparent conducting films by dispersant and chemical treatment. Journal of Materials Chemistry 18, 1261-1266.

Gu L., Zhang H., Jiao Z., Li M., Wua M. and Lei Y., 2016, Glucosamine-induced growth of highly distributed TiO_2 nanoparticles on graphene nanosheets as high-performance photocatalysts. RSC Advances 6, 67039-67048.

Joucken F., Tison Y., Le Fèvre P.,Tejeda A.,Taleb-Ibrahimi A., Conrad E., Repain V., Chacon C., Bellec A., Girard Y., Rousset S., Ghijsen J., Sporken R., Amara H., Ducastelle F. and Lagoute J. ,2014, Charge transfer and electronic doping in nitrogen-doped graphene. Scientific reports 5, 14564-14564.

Kim H.-i., Moon G.-h., Monllor-Satoca D., Park Y. and Choi W., 2011, Solar photoconversion using graphene/TiO_2 composites: nanographene shell on TiO_2 core versus TiO_2 nanoparticles on graphene sheet, The Journal of Physical Chemistry C 116, 1535-1543.

Luciu I. , 2012a, RF plasma synthesis and characterization of thin films for transparent conductors, PhD Thesis, University of Trento, Italy.

Luciu I., Bartali R. and Laidani N., 2012b, Influence of hydrogen addition to an Ar plasma on the structural properties of TiO_{2-x} thin films deposited by RF sputtering, Journal of Physics D: Applied Physics 45, 345302.

Park S., Lee K.-S., Bozoklu G., Cai W., Nguyen S.T., and S. Ruoff R. S., 2008, Graphene oxide papers modified by divalent ions - enhancing mechanical properties via chemical cross-linking, ACS nano 2, 572-578.

Park Y, Singh N.J., Kim K.S., Tachikawa T., Majima T., Choi W. , 2009, Fullerol–Titania Charge-Transfer-Mediated Photocatalysis Working under Visible Light, Chemistry - A European Journal 15(41), 10843-10850.

Safeen K., Micheli V., Bartali R., Gottardi G. and Laidani N, 2015, Low temperature growth study of nano-crystalline TiO_2 thin films deposited by RF sputtering, Journal of Physics D: Applied Physics 48, 295201.

Seo Y. S., Lee C., Lee K. H. & Yoon K. B, 2005, Charge-Transfer Complexes between Aromatic Hydrocarbons and Dry Titanium Dioxide. Angewandte Chemie International Edition 44, 910-913.

Sher Shah, M. S. A., Park A. R., Zhang K., Park J. H. and Yoo P. J., 2012, Green synthesis of biphasic TiO_2–reduced graphene oxide nanocomposites with highly enhanced photocatalytic activity, ACS Applied Materials & Interfaces 4, 3893-3901.

Speranza G. and Canteri R., 2019, RxpsG a new open project for Photoelectron and Electron Spectroscopy data processing, SoftwareX, 10, 100282.

Yang Y., Xu, L., Wang H., Wang W. & Zhang L., 2016, TiO_2/graphene porous composite and its photocatalytic degradation of methylene blue, Materials & Design 108, 632-639.

Zhang, H., Lv X., Li Y., Wang Y. and Li J, 2009, P25-graphene composite as a high performance photocatalyst. ACS Nano 4, 380-386.

Zhang Y., Tang Z.-R., Fu X. and Xu Y.-J., 2010, TiO_2_Graphene Nanocomposites for Gas-Phase Photocatalytic Degradation of Volatile Aromatic Pollutant: Is TiO_2_Graphene Truly Different from Other TiO_2_Carbon Composite Materials?, ACS Nano 4 (12), 7303 – 7314.